THE AMERICAN SOCIETY OF MECHANICAL ENGINEERS
345 E. 47 St., New York, N.Y. 10017

92-GT-33

Pressure Fluctuation on Casing Wall of Isolated Axial Compressor Rotors at Low Flow Rate

MASAHIRO INOUE, MOTOO KUROUMARU, YOUICHI ANOO

Kyushu University
Mechanical Engineering for Power
Hakozaki 6-10-1, Higashi-ku
Fukuoka, 812, Japan

ABSTRACT

The pressure fluctuations on the casing wall of two axial flow compressor rotors with various tip clearances have been analyzed by the use of two kinds of correlation functions. Behavior of the pressure fluctuation varies depending on tip clearance and blade solidity. In the case of small tip clearance, the nature of disturbances becomes random as the flow rate is reduced to a stall condition. For moderate tip clearance, coherent-structured disturbances appear intermittently at low flow rate. They appear more frequently as the solidity is increased and the flow rate becomes lower. For large tip clearance, the coherent structured disturbances exist even at considerably higher flow rates. Corresponding to these features there are peculiar patterns in the correlation designated as "phase-locked correlation function".

NOMENCLATURE

BFM = blade fluctuation moment(Eq.(4))
BPV = blade pressure variance(Eq.(5))
C_p = wall pressure coefficient
$= (\overline{p}-p_{01})/(\rho u_t^2/2)$
C_p' = pressure fluctuation coefficient
$= p'/(\rho u_t^2/2)$
f,g = pressure fluctuation component
IX = identification number of circumferential measuring point(Fig.(2))
IZ = identification number of axial measuring point (Fig.(2))
N = number of rotor revolution
$\overline{p}$ = average pressure on casing wall
p' = pressure fluctuation component
p_{01} = stagnation pressure at rotor inlet
R = time correlation coefficient
RP = phase-locked correlation coefficient
R_s = two point crosscorrelation coefficient
s = blade spacing
T,t = time
u_t = rotor tip speed
Θ,θ = circumferential coordinate
ρ = density of fluid
σ_f,σ_g = standard deviation of f, g
τ = tip clearance
ϕ = flow rate coefficient(mean axial velocity devided by u_t)
ψ = total pressure rise coefficient(total pressure rise devided by $\rho u_t^2/2$)

Subscript
1 = autocorrelation
2 = crosscorrelation

INTRODUCTION

In axial flow compressors, the investigation of aerodynamic instabilities is currently highlighted. A matter of primary concern is the fluid mechanic processes of rotating stall inception and to find a forewarning phenomenon of stall. If an occurrence of stall is foreseeable by a real-time indicator, it is possible to set a compressor operating point with a small surge margin so that it operates under high loading condition by means of a preview control technique. It would also be possible to extend the operating range by suppressing the instabilities through the use of an active control technique (Epstein et al.: 1989, Day: 1991b, Paduano et al.: 1991). These techniques are available for increasing pressure ratio per stage to reduce the total number of compressor stages.

Detailed experimental works have been made with improved measuring and analytical methods to elucidate the complex flow phenomena triggering to rotating stall. Reported so far are the existence of disturbances with different wave lengths rotating at speeds slightly lower than the rotor speed (Mathioudakis and Breugelmans: 1985), the occurrence of small stall cells travelling initially at near rotor speed and decelerating rapidly with growth in cell size (Jackson: 1987), the presence of a modal pre-stall wave propageting at a speed close to the fully developed stall cell speed(McDougall et al.:1990, Garnier et al.: 1991), and the coexistence of the formation of finite stall cells and the propagating pre-stall wave (Day: 1991a).

From a more practial point of view, the authors examined the statistical characteristics of pressure

Presented at the International Gas Turbine and Aeroengine Congress and Exposition
Cologne, Germany June 1-4, 1992
This paper has been accepted for publication in the Transactions of the ASME
Discussion of it will be accepted at ASME Headquarters until September 30, 1992

fluctuation on the casing wall of two compressor rotors with various tip clearances, and tried to find a forewarning phenomenon of rotating stall (Inoue et al.: 1991). The pseudo-space correlation maps of pressure fluctuation were drawn in the relative reference frame fixed to the rotating blades by means of the phase-locked multi-sampling data acquisition technique. According to these phase-locked patterns, it was found that the periodicity in the fluctuation with blade spacing collapsed noticeably from the maximum pressure-rise point to the stall-onset point on the overall performance characteristics. To represent the periodicity of pressure fluctuation, a practical detection parameter was proposed which was easily obtained during operation of a compressor.

However, the detection parameter requires data acquisition over 200 or more rotor revolutions, which results in deterioration of sensitivity in case of a rapid change in flow conditions. It gives no information on the instantaneous nature of the disturbance because it is a kind of statistical value.

The purpose of this study is to examine closely the nature of the disturbance prior to the stall in the previous study (Inoue et al.: 1991).

EXPERIMENTAL FACILITY

A schematic view of the rotating cascade facility in Kyushu University is shown in Fig.1. An inlet chamber (1500mm × 1500mm × 1500mm) with honeycombs and filters is installed on the upstream end of the test section. The downstream end is connected to an outlet chamber (1800mm ×1500mm × 2350mm) followed by a nozzle flow meter, a cone diffuser and an auxiliary fan. Both chambers are available to avoid a surge condition and to examine the flow behavior at stall inception. The test section consists of a fixed outer casing, a fixed journal box snd changeable assembly including a rotor, a stator, an inlet nozzle an innar casing and a hub section to provide for various cascade geometries.

Two rotors tested in this study are the same as in the previous paper (Inoue et al.: 1991). The tip diameter, hub/tip ratio and tip chord length of the blade are 449mm, 0.6 and 117.5mm, respectively for both rotors. Rotor A has low loading with low solidity of 1.25 at midspan and rotor B has high loading with high solidity of 1.67. For each rotor, the tip clearance was varied from τ =0.5mm to τ =5.0mm by changing the inner casing. Details of the geometry and blading are given in Inoue and Kuroumaru (1989).

Two high-response pressure sensors (Kulite XCQ-080-1G) were mounted on the casing wall to cover the measuring points (IZ, IX) in Fig.2 by changing the axial location and a phase-locked acquisition technique. Another set of pressure sensors is installed with an interval of 36 deg in the circumferential direction. The interval of 36 deg does not coincide with multiples of blade spacing for either rotor. An estimated error in the pressure measurement is less than 2% of the dynamic pressure corresponding to the rotor tip speed.

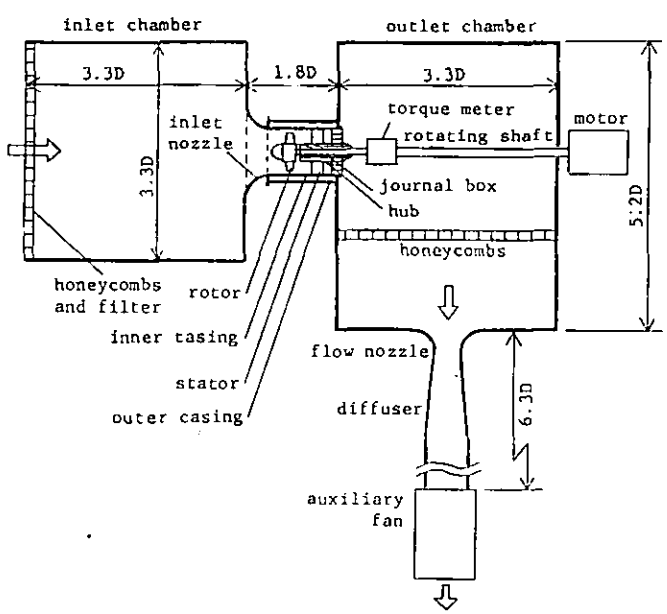

Fig.1 Low speed rotating cascade facility

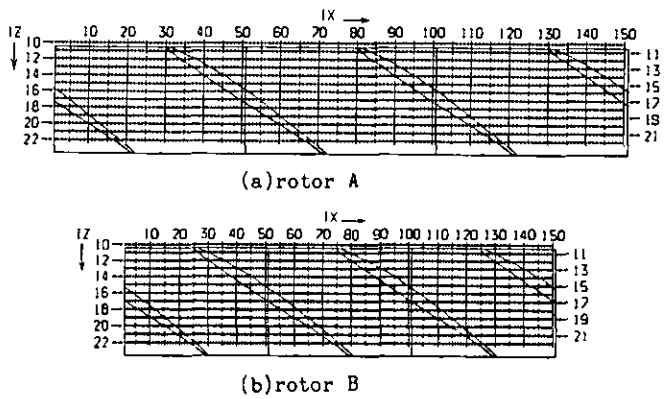

Fig.2 Measuring point in the relative frame (The circumferential and axial location of each point is identified by the numbers IX and IZ.)

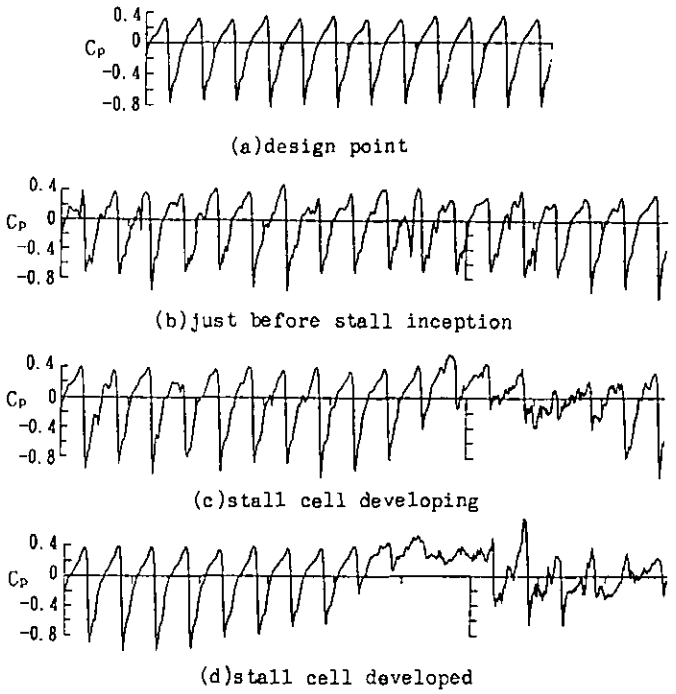

Fig.3 Typical time traces of pressure for various flow conditions (rotor A, τ=0.5mm)

TECHNICAL APPROACH

Figure 3 shows typical time traces of the pressure transducer outputs under various operating conditions. Near the design point the casing wall pressure changes regularly in the shape of saw-tooth corresponding to the blade passing. Near a stall condition small disturbances appear on the saw-toothed wave, and increase in size as the flow rate is reduced. They remain in the developing stall cell, but disappear outside the stall cell once the stall cell is fully developed. In this paper (and in the previous paper, Inoue et al.:1991), the focus is placed on this type of disturbance. It is in contrast with the approach of MIT and Cambridge University groups who focus on the disturbances of a wave length much larger than the blade spacing. In an investigation on the longer waves the blade paseing frequency waves are eliminated by a measurement upstream of the rotor or through a low pass filter. In this approach, however, the blade passing waves are eliminated by subtracting the phase-locked and averaging values from the instantaneous signals. Figure 4 is an example of the time trace of a disturbance excluding the blade passing waves.

In the previous paper, the statistical characteristics of the disturbance were clarified by the phase-locked patterns of standard deviation (pressure fluctuation), skewness and pseudo-spatial correlation in the reference frame relative to the rotating blades. An interesting feature was found in the pseudo-spatial correlation maps: under the normal flow condition the phase-locked pattern is periodic with blade spacing, but the periodicity collapses near the stall inception as shown in Fig.5. The periodic nature can easily be observed with a single pressure transducer by the cross-correlation coefficient R_s of pressure fluctuation between two points one blade spacing apart in the relative reference frame. The variations of R_s with flow rate are summarized in Fig.6 together with the performance curve, on which the hysteretic stall characteristics are indicated by dotted vertical lines : the left-hand lines correspond to the stall points with the throttle closed and the right-hand lines the stall-recovery points with the throttle opened. The correlation R_s decreases rapidly from the maximum pressure-rise point to the stall point except for the rotors with high solidity and extremely large tip clearance. For the cases with large tip clearance, the correlation R_s yields large negative values to suggest the existence of coherent structure in the disturbances which is also shown in the phase-locked spatial correlation map (Fig.5).

There are many unknown behaviors in disturbances of this type. The pseudo-spatial correlations were examined only over three blade flow passages for various tip clearances. Is there any correlation in the whole annulus ? If so, is there any relation to a long wave mode ? Does the coherent disturbance actually exist ? Does it propagate in the circumferential direction ? How does the nature of the disturbance vary with tip clearance ? In the phase-locked data acquisition, the intervals of data sampling are too large in comparison with the time scale of the disturbance, because the statistical value at each relative point is obtained by one data sampling per one rotor revolution and averaging over 200 ~ 500 revolutions. What does the pseudo-spatial correlation physically mean ? Does it have any relation to a time correlation of pressure fluctuation during one revolution of the rotor ?

A correlation function is widely used to examine the scale and propagating speed of flow disturbances. In this study, to answer the above questions, the casing wall pressure fluctuation is analyzed by two kinds of correlation functions: one is similar to that in the previous paper (Inoue et al.: 1991) and another is a common time correlation.

If f and g be the pressure fluctuations of two pressure sensors mounted on the casing at an interval of θ_p in the circumferential direction, they are functions of time t and the circumferential coordinate θ. Here, θ is measured in the relative reference frame of the rotor. A time-space correlation coefficient is written by

$$R(\Theta, T) = \overline{f(\theta, t)g(\theta - \theta_p + \Theta, t + T)}/\sigma_f\sigma_g \qquad (1)$$

where σ_f and σ_g are the standard deviations of f and g.

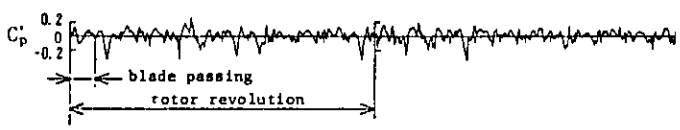

Fig.4 Time traces of pressure fluctuation excluding blade passing wave (rotor A, τ=0.5mm)

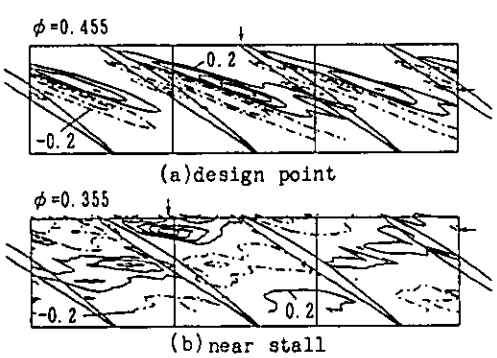

Fig.5 Phase-locked patterns of pseudo-spatial correlation at design point and near stall (rotor B, τ=2.0mm), (Inoue, et al.:1991)

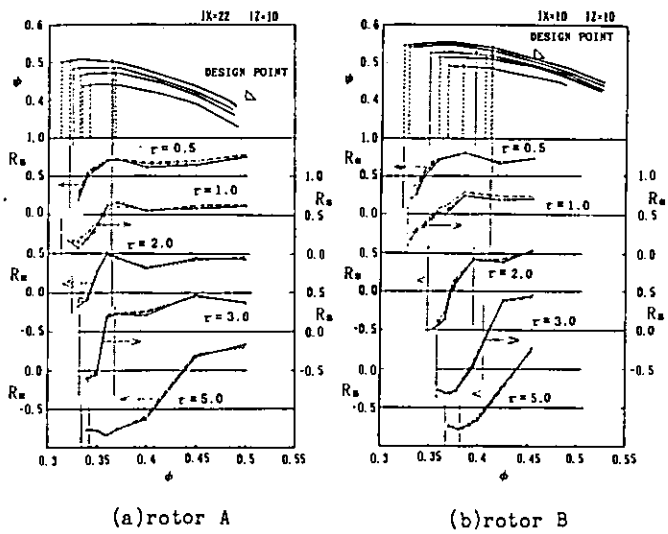

Fig.6 Variations of two-point correlation function with flow rate

$$\sigma_f = \sqrt{\overline{f^2}} \quad , \quad \sigma_g = \sqrt{\overline{g^2}}$$

In the phase-locked multi-sampling data acquisition technique, Eq.(1) is obtained as follows: (1) θ is fixed to a reference point θ_0 ; (2) Θ is changed with $\Theta = i\Delta\theta$ where i is the number of the measuring point corresponding to IX in Fig.2 and $\Delta\theta$ is the distance between two measuring points; (3)a set of f_n and g_n (suffix n denotes the number of rotor revolutions) are acquired by increasing i one by one during one rotor revolution. (4)Then, $f_n g_n$ is averaged over N rotor revolutions (N=200 ~ 500). Namely,

$$RP = R(i\Delta\theta) = \{\frac{1}{N}\sum_{n=1}^{N} f_n(\theta_o) g_n(\theta_o - \theta_p + i\Delta\theta)\} / \sigma_f\sigma_g \quad (2)$$

Equation (1) is a spatial correlation if T=0. In this technique, however, T varies with $\Theta = i\Delta\theta$ since $\Theta = \omega T = i\omega\Delta t$ (ω : angular velocity of rotor, Δt : interval of data sampling). It was called the pseudo-spatial correlation coefficient on the assumption of frozen events during sampling time in Inoue et al. (1991). The phase locked patterns in Fig.5 are obtained by placing $\theta = \theta_p$ and changing the axial location (IZ in Fig.2) of the pressure sensor of g. The correlation coefficient is unity at the reference point which is denoted by an intersection point of extensions of two arrows on the upper and right line in Fig.5. The two point crosscorrelation coefficient R_s in Fig.6 is obtained with a single pressure sensor by substituting $g=f$, $\theta_p = 0$ and a fixed interval of $i\Delta\theta = s$ (s : blade spacing) into Eq.(2). The values of IX and IZ on the upper part of Fig.6 denotes the location of reference point.

In this study, Eq.(2) is examined over a rotor revolution ($i\Delta\theta = 0 \sim 2\pi$). It is called "phase-locked correlation" because the sampling time during a rotor revolution is too long for calling it "pseudo-spatial correlation" on the assumption of frozen events. The phase-locked autocorrelation coefficient with $g=f$ and $\theta_p = 0$ is denoted by RP_1 and the phase-locked cross correlation coefficient with θ_p =36 deg by RP_2 .

On the other hand, Eq.(1) is a time correlation in the absolute frame of the casing. By means of the multi-sampling technique without phase-lock, it can be obtained by replacing t and T by $j\Delta t$ and $i\Delta t$.

$$R = R(i\Delta t) = \{\frac{1}{M}\sum_{j=1}^{M} f(j\Delta t) g(i\Delta t + i\Delta t)\} / \sigma_f\sigma_g \quad (3)$$

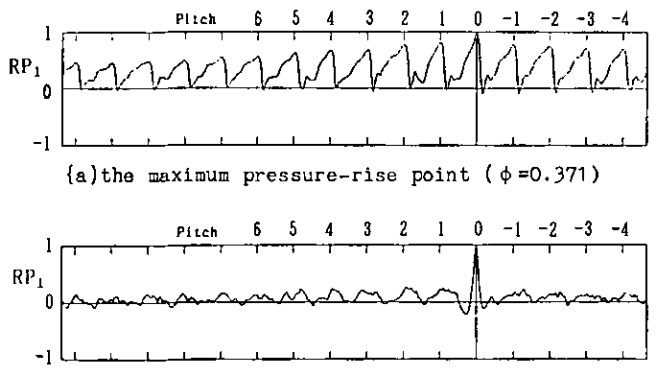

(a)the maximum pressure-rise point (ϕ =0.371)

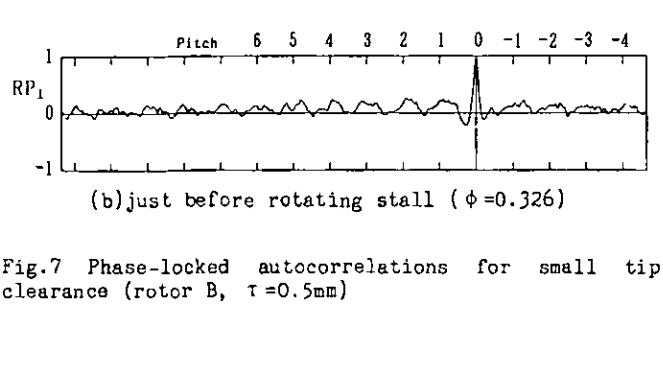

(b)just before rotating stall (ϕ =0.326)

Fig.7 Phase-locked autocorrelations for small tip clearance (rotor B, τ =0.5mm)

where M is the total sampling numbers acquired during several blade passing period. The autocorrelation coefficient denoted by R_1 is obtained with a single sensor by substituting $g=f$ into Eq.(3). The crosscorrelation coefficient denoted by R_2 is obtainad with two sensors 36 deg apart from each other.

These correlations are mainly investigated on the casing wall near the rotor leading edge (IZ=10 or 12 in Fig.2).

EXPERIMENTAL RESULTS AND DISCUSSION

Rotors with small tip clearance Figures 7 and 8 show the typical phase-locked autocorrelations RP_1 and the phase-locked crosscorrelations RP_2 in the case of small tip clearance (τ =0.5mm). The short vertical lines on the upper and lower frame line indicate the relative distance from a reference point ($\theta = \theta_0$) with multiple of blade spacing. The vertical dotted lines in Fig.8 are multiples of distance between two sensors. As the distributions of RP_1 and RP_2 at design point were essentially similar to those at the maximum pressure-rise point in the case of small tip clearance, the latter is compared with the correlation just before the stall inception in the figures. The data just before the rotating stall were obtained by a pretrigger data acquisition system by Inoue et al.(1991), in which a required number of the data samples before a trigger of stall inception are acquired in a micro-computer. The trigger pulse of stall inception is taken by setting a threshold level for the low pass filtered signal of a pressure sensor.

The phase-locked correlation RP_1 and RP_2 are periodic with blade spacing at the maximum pressure-rise point. This phenomenon suggests that the time scale of dominant disturbances is the same order or considerably large in comparison with the time of one rotor revolution. As the fluctuation level is very low in the case of small tip clearance under the normal flow condition, this behavior of disturbances may be due to variations in tip clearance or fluctuations in inlet or outlet conditions.

The periodicity of RP_1 and RP_2 rapidly degenerates toward stall and nearly disappears just before stall inception due to the appearance of random disturbances with high amplitude. It is shown in Fig.7(b) that the scale of the disturbance is less than half of the spacing. There is no evidence indicating the propagation of disturbance in the RP_2 correlation (Fig.8(b)).

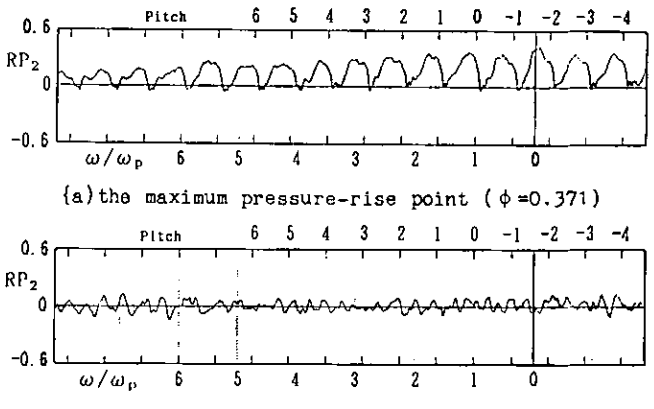

(a)the maximum pressure-rise point (ϕ =0.371)

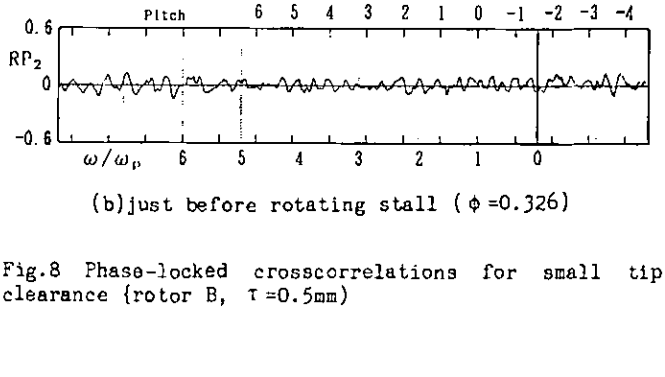

(b)just before rotating stall (ϕ =0.326)

Fig.8 Phase-locked crosscorrelations for small tip clearance (rotor B, τ =0.5mm)

Figures 9 (a) and (b) show the variation of the autocorrelation with the numbers of rotor revolutions. Figure 9(a) is at the maximum pressure-rise point, Fig. 9(b) is several revolutions before the trigger of stall inception. In Fig.9(b), the trigger pulse is taken at N=520 under the fixed throttle condition. In each case, the average over 20 revolutions is shown on the lowest line. The intervals of vertical dotted lines correspond to blade spacing. In the case of maximum pressure-rise, R_1 is periodic with blade spacing for most of the revolutions. Just before rotating stall, there are a few cases where R_1 is periodic, but over most of the rotation, the time correlation is weak and random, which results in disappearance of correlation in the average case. No essential difference was found in R_1 between 500 and several revolutions before the stall inception (Figure is omitted).

The crosscorrelation R_2 of two sensors 36° apart from each other is also examined. Just before the stall inception, appreciable correlation was hardly seen over each revolution, and there was no correlation in the average of 20 revolutions as shown in Fig.10 (a). Figure 10 (b) is only one case tested where a coherent structure appears in R_2 for the small tip clearance. There are only two revolutions before the stall trigger pulse. In this case, a stall inception cell smaller than the trigger threshold was observed in the low pass filtered signal of the pressure sensor.

There seems to be no coherent disturbance before the stall inception in the case of small tip clearance. The stall inception cell appears without any

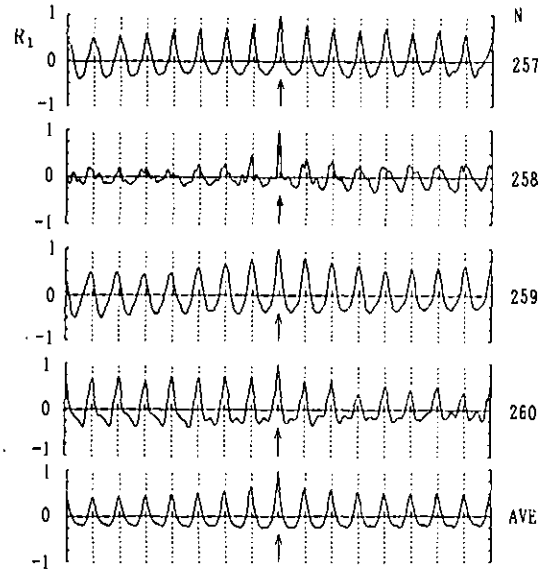

(a)the maximum pressure-rise point (ϕ =0.371)

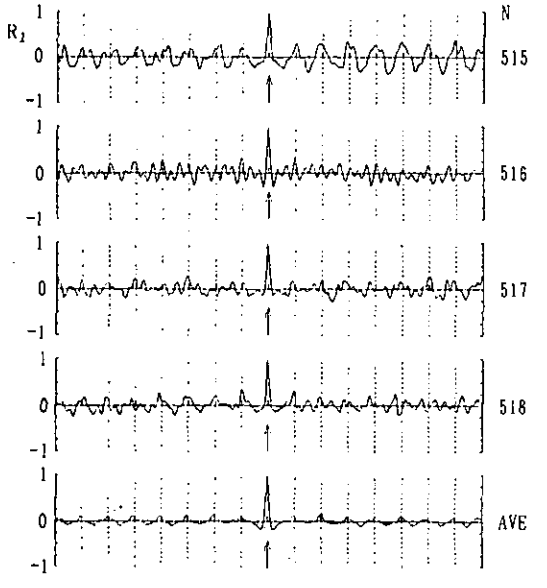

(b)just before rotating stall (ϕ =0,326)

Fig.9 Time autocorrelations for small tip clearance (rotor B, τ =0.5mm)

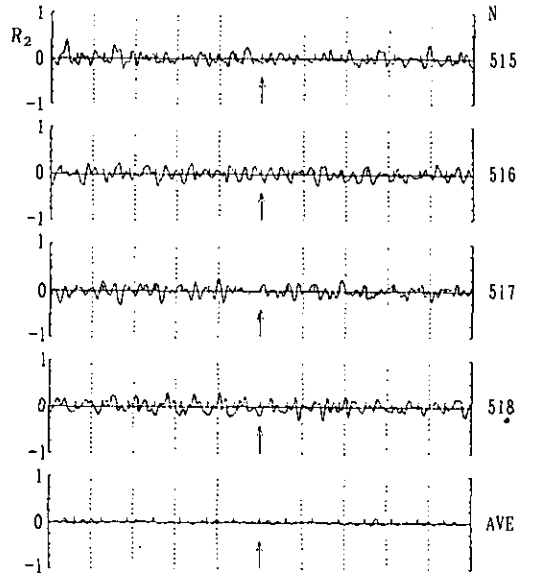

(a)rotor B, τ =0.5mm

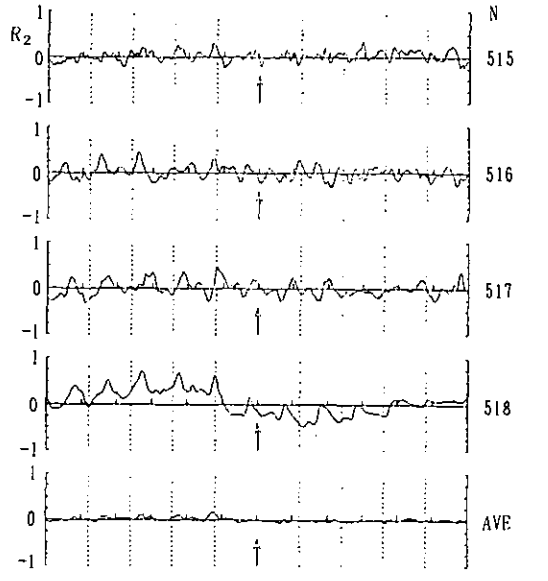

(b)rotor A, τ =0.5mm

Fig.10 Time crosscorrelations just before stall inception for small tip clearance

forerunner and grows rapidly. If the periodicity of correlation with blade spacing disappears, it is likely that a small stall cell will appear.

Rotor with moderate tip clearance In the case of moderate tip clearance (τ =2.0mm), the phase-locked correlations RP_1 and RP_2 are periodic over the whole relative circumference at the design flow rate (Figures are omitted). As the flow rate decreases, the periodicity of RP_1 and RP_2 degenerates and collapses at the maximum pressure rise point as shown in Figs.11 (a) and 12 (a). This behavior is smilar to that just before the stall inception in the small tip clearance. In the RP_2 correlation, however, a considerably higher value appears near a location of 2 on the abscissa. If the disturbance at the position of sensor f had moved with the blade, RP_2 would become high at the location of 0 in Fig.12 (a). The high values at the location of 2 suggests the existence of disturbances rotating at 44% speed of the rotor speed in the circumferential direction.

A clearer coherent structure of the disturbances is found in the RP_1 correlation just before the stall inception (Fig.11(b)). This structure makes the two point cross correlation R_s negative as shown in Fig.6. The comparisan of the RP_1 and RP_2 correlation indicates that the disturbances rotate in the circumferential direction at 46% of the rotor speed.

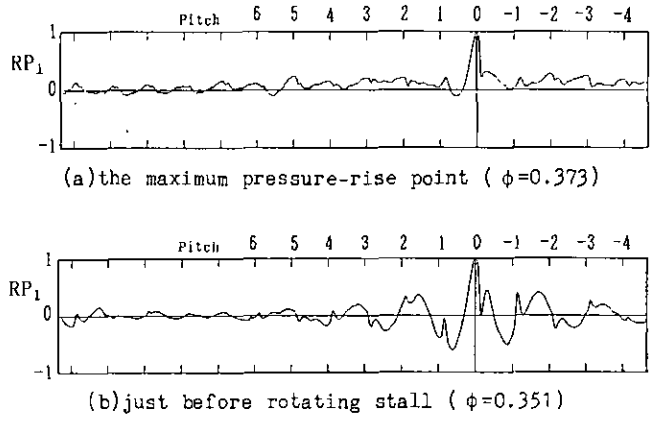

Fig.11 Phase-locked autocorrelations for moderate tip clearance (rotor B, τ =2.0mm)

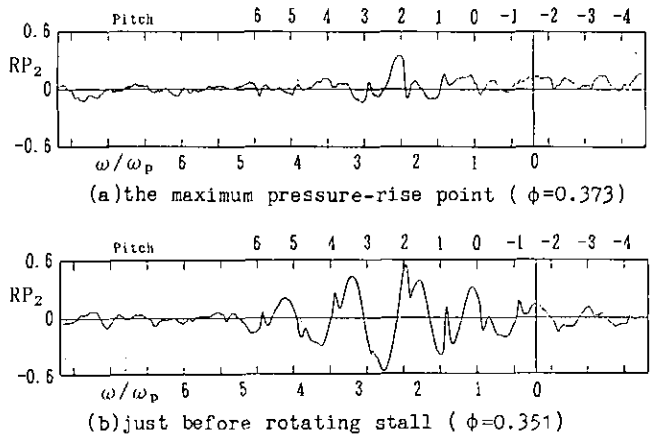

Fig.12 Phase-locked crosscorrelations for moderate tip clearance (rotor B, τ =2.0mm)

This phenomenon can be observed in shorter time scale (order of a rotor revolution) by means of the time correlations R_1 and R_2. Figures 13 (a) and (b) are the variation of the autocorrelation R_1 with the rotor revolution at the maximum pressure-rise point and just before the stall inception. At the maximum pressure rise point, various types of the R_1 correlation are observed depending on the number of rotor revolutions: periodic nature with blade spacing (N=265), random nature of small disturbance (N=264, 266) and coherent nature of larger scaled disturbance (N=263). Averaging these distributions, the resultant correlation is simlar to the phase-locked autocorrelation in Fig.11. Near the stall condition, the R_1 correlation indicates the nature of larger

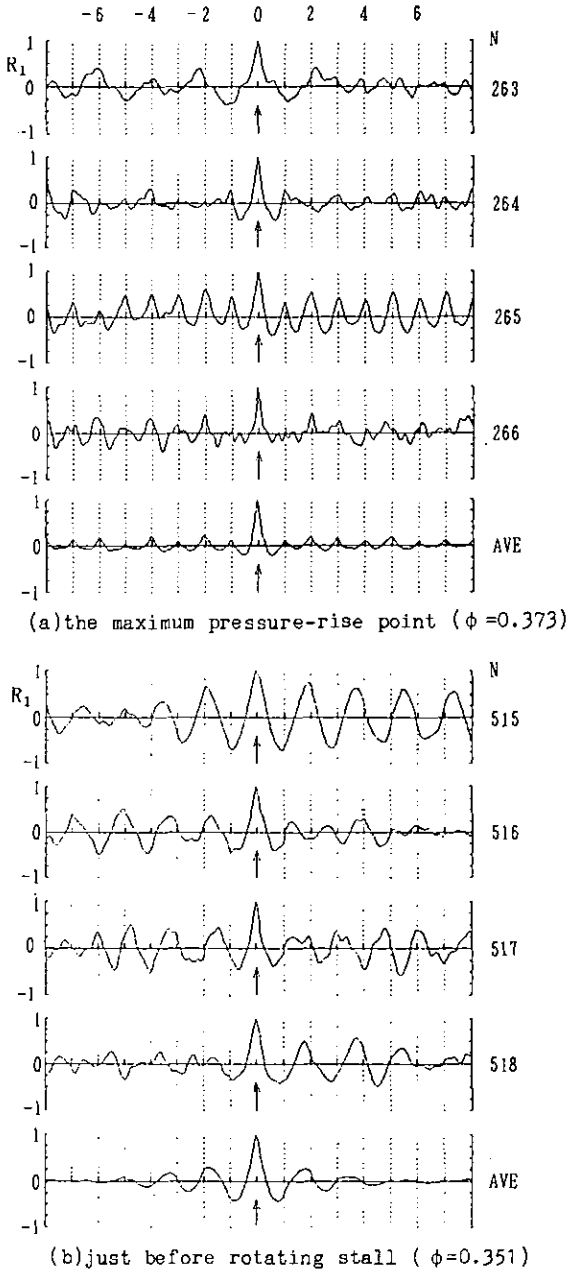

Fig.13 Time autocorrelations for moderate tip clearance (rotor B, τ =2.0mm)

scaled disturbances in comparison with the blede spacing for elmost all revolutions. If the disturbance rotates in the circumferential direction, its speed is about a half of the rotor speed judging from the number of the peaks. As the interval of ths R_1 pseks differs a littls depending on rotor revolution, the averaged correlation becomes weaker with the relative distance from the reference point, and is similar to the phase-locked autocorrelation in Fig. 12(b).

Figures 14 is the variation of the crosscorrelation R_2 just before the stall inception. The dietributions are similar to those of the R_1 correlation. In each revolution, the rotating speed of the disturbance cannot be estimeted becauss it is difficult to find which peaks correspond to sach other between R_1 and R_2 . However, averaging the R_2 correlation, the peaks of R_2 indicates the existence of dominant rotating speed which coincides with the speed estimated by the phase-locked correlations. At the maximum pressure-rise point, both the random mode in Fig.10 and the coherent mode in Fig.14 appear depending on rotor revolution (Figure is omitted). The averaged R_2 correlation was similar to the phase-locked crosscorrelation in Fig.12(b).

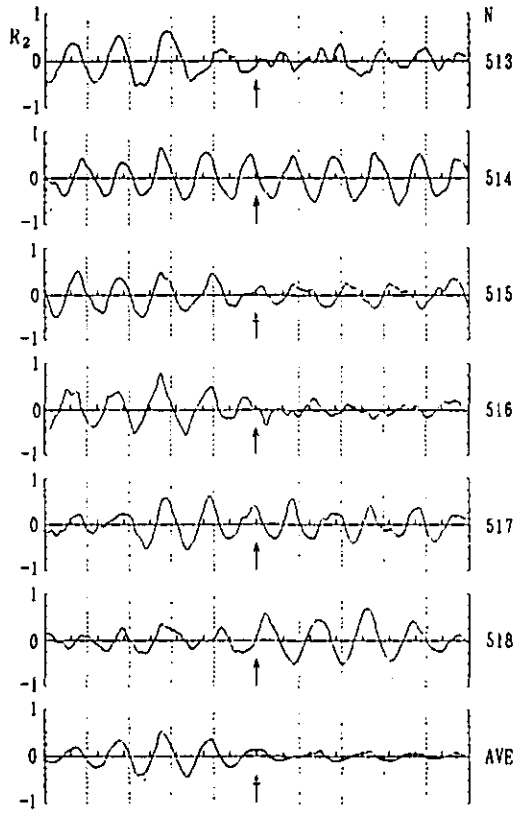

Fig.14 Time crosscorrelations just before stell inception for modsrate tip clearance (rotor B, τ =2.0mm)

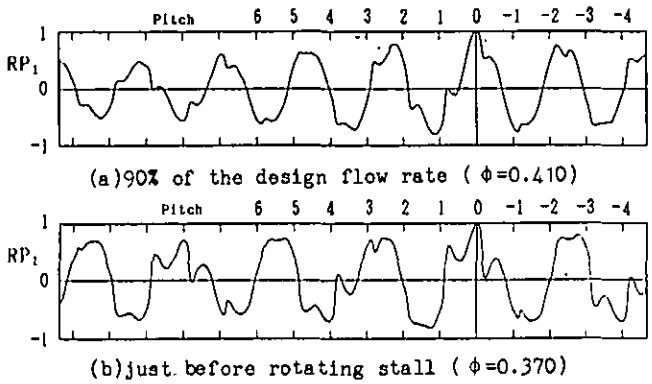

Fig.15 Phase-locked autocorrelation for large tip clearance (rotor B, τ =5.0mm)

Rotor with large tip clearance In the case of the largest tip clearance, the performance deteriorates noticeably because the clearance is 4.3% of chord

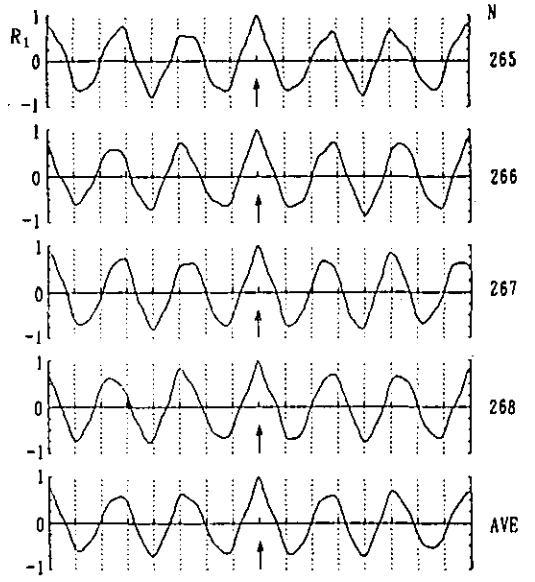

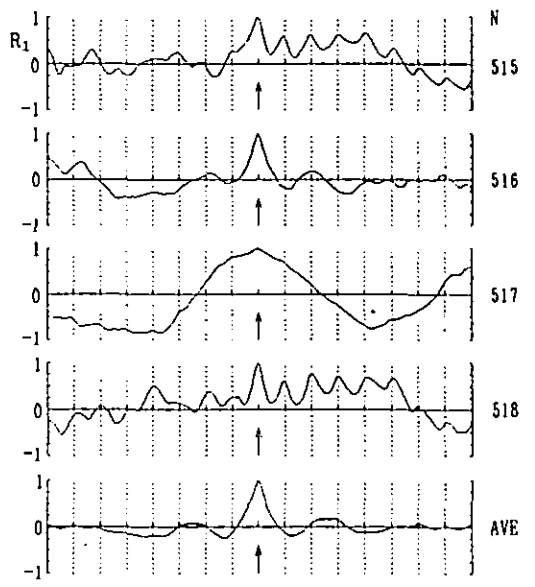

Fig.16 Time autocorrelation for large tip clearance (rotor B, τ =5.0mm)

length and 5.1% of blade span. The measurements for these rotors were made not for practical purpose but for physical interest. At the design point, the periodicity with blade spacing is appreciable in the phase-locked correlation. But it collapses at flow rates considerably higher than that for the maximum pressure-rise point. Instead, the large scaled disturbances appear in the RP_1 correlation as shown in Fig.15(a). As a result, two point correlation R_s becomes negative at considerably high flow rate as shown in Fig.6. The scale of disturbances changes little as the flow rate is reduced to the stall point value as shown in Fig.15(b), and is 2 ~ 2.3 times the blade spacing. The time correlation R_1 is similar to the phase-locked correlation RP_1 for each revolution as , shown in Fig.16 (a). The rotating speed of the disturbances is estimeted to be 40 ~ 50%. This nature of the disturbances exists about 100 revolutions before the stall inception (Figure is omitted). However, the new type of disturbance appears about 20 revolutions before the stall. As shown in Fig.16 (b), it turns into a long wave mode length which is of the order of the circumferential length of the annulus.

Additional Discussions The phase-locked patterns of the statistical characteristics of pressure fluctuation presumed the occurrence of intermittent local separation at the leading edge near the stall condition (Inoue et al.: 1990 and 1991). There is experimental evidence to support this presumption. In order to examine a fluctuating condition in each blade flow passage, the blade fluctuation moment (BFM) and the blade pressure variance (BPV) are defined as

$$BFM = \overline{p'(\theta - s/2)} / (\rho u_t^2 s / 2) \qquad (4)$$

$$BPV = \overline{(p')^2} / (\rho u_t^2 / 2)^2 \qquad (5)$$

where p' is the pressure fluctuation component shown in Fig.4 and a bar indicates the average from suction side to pressure side in a blade flow passage at a fixed axial location. When the instantaneous circulation (proportional to lift force) is higher (or lower) than the average, the pressure is higher (or lower) on the pressure side and/or lower (or higher) on the suction side, then, the BFM is positive (or negative). The BPV value is high in a blade flow passage with large disturbances. Figure 17 shows the variation of BFM and BPV just before the stall inception in the case of moderate tip clearance. Near stall, the flow passages with high negative BFM appear intermittently due to the leading edge separation. It is found from Fig.17 that BPV becomes high in the same flow passage with negative BFM. That is, the large disturbance is caused by the intermittent local separation of the blade. Occurrence of the local separation is quite irregular. The frequency of the occurrence increases as stall inception is approached. A small stall cell develops abruptly from one of them.

There seem to be two types of disturbances which collapse the periodic nature with blade spacing at low flow rate. One is a small scaled random disturbance which appears mainly in the case of small tip clearance. Another is a larger scaled coherent-structured disturbance appearing even at considerably higher flow rates in the case of large tip clearance. In the case of moderate tip clearance, both types of disturbances coexist. The frequency with which the coherent-structured disturbances appear increases as the tip clearance becomes large. It increases also as the solidity is increased. This is probably related to accumulation of low energy fluid in the tip

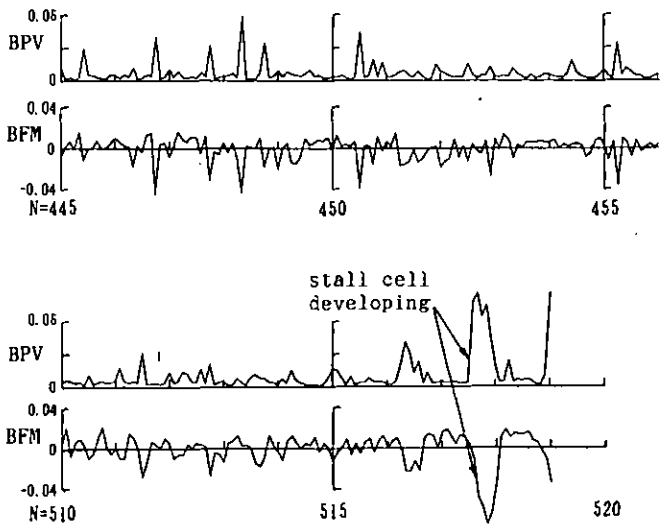

Fig.17 Variation of blade fluctuation moment and blade pressure variance with rotor revolution (rotor A, τ =0.5mm)

region. The low energy fluid blocks the blade flow passages near the tip. The accumulation is severe for large tip clearances and low flow rates. A rotor with high blade solidity is likely to be blocked by the low energy fluid. It makes the casing wall boundary layer thick and tends to change the thickness along the circumference of casing wall (McDougall et al.: 1990). Does the coherent-structured disturbance form in this condition ? If so, the tip clearance may not be the only parameter. The inlet boundary layer thickness may be an important parameter as well. Blade loading distribution also affects this behavior because the intermittent local separation near the leading edge brings about the accumulation of low energy fluid due to the centrifugal force. The effects of these parameters should be investigated in the future.

The estimated rotating speed of the coherent-structured disturbance was 40% to 50% of the rotor speed in this experiments. On the other hand, the rotating speed of the stall cell was 64% to 68% in all the cases tested.

An attempt was made to find a long pre-stall wave which was found upstream of the rotor investigated by McDougall et al. (1990) and Garnier et al. (1991). In the present study, the signals from two pressure sensors 36 deg apart from each other were examined through a numerical low pass filter. In some cases for short time length, the disturbances rotating near 50% of rotor speed were appreciable. However, the low pass filtered signals were too noisy to obtain sufficient evidence of the wave. In the present stage, it is not clear that the coherent-structured disturbance in this experiment is directly related to the long pre-stall wave. But, it is probable that the coherent-structured disturbance affects the fluctuation upstream of the rotor.

CONCLUSIONS

The casing wall pressure fluctuation of two axial flow compressor rotors with various tip clearance has been investigated. The regular saw-toothed pressure fluctuation due to blade passing is removed by subtracting the phase-locked ensemble average of pressure. The fluctuation component excluding the blade passing wave has been analyzed by the use of two

kinds of correlation functions. One is ths statistical function in the reference frame relative to rotating blades, and designated as "phase-locked correlation function" which ie obtained by phase-locked multi-sampling data acquisition during several hundred revolutions of rotor. Another is a common tims correlation function which is obtained in each rotor revolution. The results are summarized ae follows:

1. A pattern of the phase-locked correlation function variss depending on flow rate, tip clearance and solidity. This is closely related to the nature of the disturbancss.
2. There are two typss of disturbances at low flow rate. One is of random disturbances appearing in the case of small tip clearance, and another is of coherent-structured disturbances appearing even at considerably higher flow rates in the case of large tip clearance.
3. In the cass of moderate tip clearance, both types of disturbances coexist at low flow rate. The frequency with which the coherent-structured disturbances appear increases as ths tip clearance becomes large and the solidity is increased.
4. For small and moderate tip clearances, the psriodicity of the correlation function with blade spacing decreases noticeably as the flow rate is reduced to the stall point value. This is due to the random disturbances with large amplitude produced by intermittent local separation at blade leading edge.
5. The coherent-structured disturbances rotate in the circumferential direction. In this experiment, the rotating speed was 40 ~ 50% of the rotor speed which was different from the rotating speed of the stall cell.

ACKNOWLEDGMENT

The authors appreciete the assistance of Messrs. S. Higuchi end H. Ugajin during the experimental work. They also gratefully acknowledge the financial support of Grant in Aid for Scientific Research (B) of The Ministry of Educstion, Science and Culture, and of Harada Memorial Foundation.

The first author is extremely grateful to Dr. I. J. Day for useful discussions in his short stay in Cambridge, and to Prof. N. A. Cumpsty for inviting him to Cambridge. He is also appreciative of the useful information from Prof. E. M. Greitzer.

REFERENCES

Day, I. J., 1991a, "Stall Inception in Axial Flow Compressors", ASME Paper, 91-GT-86.

Day, I. J., 1991b, "Active Suppression of Stall and Surge in Axial Flow Compressors", ASME Paper 91-GT-87.

Epstein, A. H., Flowes Williams, J. E., Greitzer, E. M., 1989, "Active Suppression of Aerodynamic Instabilities in Turbomachinery, Journal of Propulsion and Power, Vol.5, No.2, 1989, pp.204-211.

Garnier, V. H., Epstein, A. H., Greitzer, E. M., 1991, "Rotating Waves as a Stall Inception Indication in Axial Compressors", ASME Journal of Turbomachinery, Vol.113, No.2, pp.290-301.

Inoue, M., Kuroumaru, M., 1989, "Structure of Tip Clearance Flow in an Isolatsd Axial Compressor Rotor", ASME Journal of Turbomachinery Vol.111, No.3, pp.250-256.

Inoue, M., Kuroumaru, M., Ando, Y., 1990, "Behavior of Tip Clearance Flow in an axial Flow Impeller at Low Flow Rate, Proceedings of ths 3rd China-Japan Joint Conference of Fluid Machinery, Vol.2, pp.179-186.

Inoue, M., Kuroumaru, M., Iwamoto, T., Ando, Y., 1991, "Dstection of Rotating Stall Prscursor in Isolated Axial Flow Compressor Rotors", ASME Journal of Turbomachinery, Vol.113, No.2, pp.281-287.

Jackson, A. D., 1987, "Stall Cell Development in an Axial Gompressor", ASME Journal of Turbomachinery, Vol.109, No.4, pp.492-498.

Mathioudakis, K., 8reugelmans, F. A. E., 1985, "Development of Small Rotating Stall in a Single Stage Axial Compressor" ASME Paper, 85-GT-227.

McDougall, N. M., Cumpsty, N. A., and Hynes, T. P., 1990, "Stall Inception in Axial Compressors, ASME Journal of Turbomachinery, Vol.112, No.1, pp.116-125.

Paduano, J., Epstein, A. H., Valavani, L., Longlei, J. P., Greitzer, E. M., Guenette, G. R., 1991, "Active Control of Rotating Stall in a Low Speed Axial Compressor, ASME Paper, 91-GT-88.